Title
Intestinal subepithelial myofibroblasts support the growth of Lgr5 stem cells

Author
Lei, Nan Ye

Publication Date
2012

Peer reviewed|Thesis/dissertation

UNIVERSITY OF CALIFORNIA

Los Angeles

Intestinal subepithelial myofibroblasts support the growth of Lgr5 stem cells

A thesis submitted in partial satisfaction

of the requirements for the degree Master of Science

in Biomedical Engineering

by

Nan Ye Lei

2012

ABSTRACT OF THE THESIS

Intestinal subepithelial myofibroblasts support the growth of Lgr5 stem cells

by

Nan Ye Lei

Master of Science in Biomedical Engineering

University of California, Los Angeles, 2012

Professor James Dunn, Chair

Intestinal epithelial stem cells (IESC) have been an area of intense study for applications in tissue engineering and understanding intestinal diseases. Feeder support cells are used in a variety of stem cell co-cultures to sustain their growth. Intestinal subepithelial myofibroblasts (ISEMF) are the natural support cells for intestinal stem cells *in vivo*. In this study, IESC and were grown in co-culture with ISEMF in the in vitro and in vivo setting. We showed that ISEMF enhanced the growth of IESC *in vitro* and were critical for the formation of intestinal epithelial structures *in vivo*. ISEMF supported the growth of intestinal crypts *in vitro* even in the absence of added soluble Rspo1. This co-culture system reconstitutes a part of the intestinal stem cell niche.

The thesis of Nan Ye Lei is approved.

Ben Wu

Min Lee

James Dunn, Committee Chair

University of California, Los Angeles

2012

TABLE OF CONTENTS

ACKNOWLEDGEMENTS

I would like to thank the co-authors Jiafang Wang, Vaidehi Joshi, Ziyad Jabaji, R. Sergio Solorzano-Vargas, Artur Jaroszewicz, Stephanie C. Tung, Connie Martin, and Michael Lewis and the principle investigators Matthias Stelzner, James Dunn, and Martin Martin for their contributions to this work. It is currently in preparation for publication.

This work was supported by grants from the National Institute of Diabetes and Digestive and Kidney Diseases U01 Intestinal Stem Cell Consortium (DK085535-01 and DK085535-02S2), DK083762, and DK083319.

Introduction

Intestinal epithelial stem cells (IESC) have recently been a field of concentrated research. Many of the publications have focused on identifying markers for the stem cell populations and the biomolecular pathways that determine the fate of the stem cells. (1, 2) Lgr5 has been identified as an unique marker for these stem cells (3) and subsequent work has shown single sorted Lgr5 expressing cells are capable of regenerating the intestinal epithelial lineages *in vitro* (4). Lgr5 is a Wnt target gene and the Wnt pathway is responsible for intestinal epithelial growth and differentiation (5). Wnt agonists are required to drive the pathway for stem cell survival and proliferation and consequently the Wnt agonist R-spondin1 (Rspo1) has been added to the culture medium in all reported *in vitro* systems (4, 6).

Feeder cells have been used in embryonic stem cell culture and are vital in co-cultures without an established matrix (7). Intestinal epithelial myofibroblasts (ISEMF) are found adjacent to the crypts *in vivo* and may serve as feeder cells for the culture of IESC. Previous studies have shown that ISEMFs have a role in epithelial growth and differentiation and wound healing in the intestine (8). The exact mechanism for these effects is unknown, but it is believed to be due to secreted growth factors from the ISEMF.

It is of interest to analyze the effect of ISEMF on intestinal epithelial cells to better understand the stem cell niche and to assess potential beneficial effects on growth. Current IESC *in vitro* cultures require multiple added growth factors and it has been suggested that some of these growth factors are derived from the neighboring Paneth cells (9), while others are likely derived

from ISEMF (10). In a co-culture system, the ISEMF may provide some of the necessary factors for stem cell survival. This would be especially relevant in the *in vivo* setting where exogenous growth factors cannot be easily delivered. Moreover, ISEMF constitute an important element of the intestinal stem cell niche and additional knowledge of the cells will be useful for future clinical applications. In particular, intestinal tissue engineering, a potential therapy for short bowel syndrome, would require components from the epithelial, submucosal, and muscular layers to create a fully functional construct. Understanding the interactions between these cells would allow for a better model in designing the engineered intestine.

In this study, we examined the effect of ISEMF on the growth of intestinal epithelial cells in a co-culture system and *in vivo*. In the *in vitro* setting, IESC were grown either in direct contact with ISEMF or separated from ISEMF by a semi-permeable membrane to examine the effect of distance on their interaction. The cultures were also implanted subcutaneously to determine their *in vivo* viability. The growth and differentiation of intestinal epithelial cells were assessed both *in vitro* and *in vivo* through size measurements, DNA and RNA quantitative real-time PCR, and immunohistochemistry. We also used RNA deep sequencing to identify overexpressed genes unique to ISEMF that may be translated to growth factors responsible for their effects. ISEMF were transduced with short hairpin RNA to silence expression of those genes and confirm their role in normal ISEMF.

Methods

Animal Usage

Animal usage complied with institutional regulations set by the Animal Research Committee at the University of California, Los Angeles. C57BL/6-Tg(Actb-EGFP)1Osb/J (GFP) (The Jackson Laboratory, Bar Harbor, Maine) and B6.129P2-*Lgr5*$^{tm1(cre/ERT2)Cle}$/J (Lgr5-GFP) (The Jackson Laboratory) mice were bred at the UCLA Division of Laboratory Animal Medicine under standard conditions. Wild type C57BL/6 mice were purchased from Charles River (Wilmington, MA).

ISEMF isolation and culture

ISEMF were isolated using a modified protocol for isolating intestinal organoids. (11) Five-day old wild type C57BL/6 neonates were euthanized by isoflurane and decapitation. The entire small intestine was removed, submerged in cold HBSS* (Hank's Buffered Salt Solution without calcium and magnesium (Invitrogen, Carlsbad, CA) with 2% D-glucose (Sigma, St. Louis, MO), penicillin-streptomycin (Invitrogen), and L-glutamine (Invitrogen)), and diced into 1 mm^2 pieces with a razor blade. The diced pieces were washed three times with HBSS* before being transferred into HBSS* with 0.125 U/mL dispase type I (Invitrogen) and 300 U/mL collagenase type XI (Sigma) and allowed to incubate for 25 minutes at room temperature. The digested tissue was vigorously shaken for 30 seconds, allowed to gravity sediment for 1 minute, and the supernatant was collected. This was repeated 3 times and then DMEM-S (Dulbecco's modified

eagle medium high glucose (Invitrogen) with 5% fetal bovine serum (FBS, Invitrogen), 2% D-sorbitol (Sigma), penicillin-streptomycin, and L-glutamine) was added and the collected supernatant was centrifuged at 100 g for 2 minutes. The pellets were pooled, resuspended in DMEM-S, and centrifuged. The washed pellet was resuspended in DMEM-S and allowed to gravity sediment for 3 minutes. The supernatant was collected and the pellet was collected at 2 minutes of gravity sedimentation. The pellet was resuspended in HBSS Rinse (HBSS with calcium and magnesium (Invitrogen) with penicillin-streptomycin and L-glutamine) and gravity sedimented for 3 minutes before the supernatant with the organoids was collected. The organoids were plated at 5000 per milliliter of ISEMF media(12), DMEM with 10% FBS, 0.25 U/mL insulin (Sigma), 10 µg/mL transferrin (Sigma), and 20 ng/mL epidermal growth factor (EGF, Peprotech, Rocky Hill, NJ) into a T25 flask. ISEMF cells attached to the flask and formed colonies after 3 days and were subsequently passaged and expanded following normal cell culture technique.

Intestinal crypt isolation

Small intestinal crypts were isolated using a modified version of the protocol described by Sato et al.(4). Briefly, the small intestine from a 6-10 week old GFP mouse was removed, inverted, and scraped with a hemocytometer coverslip to remove villi. The intestine was cut into 0.5 cm pieces, washed 3 times with phosphate buffered saline (PBS, Invitrogen), and placed in a 2.5 mM EDTA (Sigma) solution for 30 minutes at 4°C. The resulting tissue was vortexed 10 times in 3 second pulses and the supernatant was collected. This was repeated to obtain 6 fractions and they were centrifuged at 100 g for 2 minutes. The pellets were resuspended in 2 mL of PBS with

10% FBS and were examined under a light microscope to determine the fraction with crypts. The selected fractions were pooled, filtered through a 100 µm and 70 µm cell strainer (BD Biosciences, Franklin Lakes, NJ) and centrifuged at 100 g. The pellet was resuspended in 5 mL of Basic Crypt Media (Advanced DMEM/F-12 (Invitrogen) with penicillin-streptomycin, Glutamax (Invitrogen), and HEPES (Invitrogen)) and centrifuged again to obtain intestinal crypts.

The crypts were plated in Matrigel (BD Biosciences) at a concentration of 250 crypts per 25 µL of Matrigel in a 48-well plate. In the control group without ISEMF, the crypt-Matrigel suspension was placed directly in the well. For study group with crypts on top of ISEMF, crypts in Matrigel were placed on a monolayer of 25,000 ISEMF that were cultured in the gelatin-coated well the day before. In the study where crypts were mixed with ISEMF in Matrigel, crypts were mixed with 25,000 ISEMF in Matrigel and placed in the well. In the membrane separation experiments, 500 crypts in 50 µL of Matrigel were placed on a cell culture membrane insert hanging on a 24-well companion plate (BD Biosciences) with either 50,000 ISEMF or no cells in the well below the membrane. Complete Crypt Medium (Basic Crypt Medium with N2 (Invitrogen), B27 (Invitrogen), 50 µg/mL EGF, 1 mM N-acetylcysteine (Sigma), 100 ng/mL noggin (Peprotech), and 1 µg/mL R-spondin1 (Rspo1, R&D Systems)) was overlaid on the cultures after the Matrigel solidified. Fresh EGF, noggin, and Rspo1 supplements were added every 2 days, and the entire culture medium was changed every 4 days.

Single cell isolation and FACS

Single cells were obtained for stem cell sorting following a previously described method.(6) Briefly, the jejunum of a Lgr5-GFP mouse was dissected, cut open, and cleaned before it was placed in PBS with 30 mM EDTA, 1.5 mM DTT (Sigma), and 10 µM Y-27632 (Sigma) on ice for 20 minutes. Subsequently, the tissue was transferred into PBS with 30 mM EDTA and 10 µM Y-27632 and incubated for 8 minutes at 37°C. The tissue was shaken at 2.5 shakes per second to dissociate the epithelium and the suspension of epithelium was centrifuged at 1000 g for 5 minutes. The pellet was incubated in HBSS with 0.3 U/mL dispase for 10 minutes and was shaken at 3.5 shakes per second every 2 minutes to avoid clumping. FBS and DNase were added to the solution to make it 10% FBS and 100 U/mL DNase (Sigma) in concentration and then filtered through 70 µm and 40 µm cell strainers. The cells were centrifuged and resuspended in HBSS twice prior to antibody staining.

For *in vitro* and *in vivo* implant histology, the cells were stained with PE annexin V (Invitrogen), propidium iodide (PI, Invitrogen), PE/Cy7 CD 31 (Biolegend, San Diego, CA), PE/Cy7 CD45 (Biolegend), eFluor 450 EpCAM (E-Bioscience, San Diego, CA), and APC CD44 (Biolegend). They were also stained for their corresponding isotype antibody as negative controls. The cells were sorted by a BD FACSAria (BD Biosciences) cell sorter. The gates were set up to exclude the doublet cells and annexin V, PI, CD31, and CD45 positive populations. The CD44 and Lgr5-GFP double positive population was collected into Complete Crypt Medium with 10 µM Y-27632. The cells were pelleted, mixed in Matrigel at 500 to 3000 cells per 15 µL, and plated in a 96-well plate on top of or without ISEMF. Complete Crypt Medium with 10 µM Y-27632 and 100 ng/mL Wnt3a (R&D Systems) was overlaid on the cultures after the gels have solidified.

Fresh EGF, noggin, Rspo1, and Wnt3a were added every 2 days and the medium was changed every 4 days.

Single sorted cells used in the growth measurement experiments were stained for 7-AAD and APC Annexin V. The cells were sorted by a BD FACSAria cell sorter. The gates selected for single cells then live cells negative for 7-AAD and Annexin V and finally GFP positive Lgr5 stem cells. The cells were collected into Complete Crypt Medium with 10 µM Y-27632. The cells were pelleted and resuspended in 15 µL per 800 cells of Matrigel containing 750 ng/mL EGF, 1.5 µg/mL Noggin and 15 µM Jagged-1. 15 µL of the suspension was plated in a 96-well on top of or without ISEMF. The plate was incubated at 37°C for 15 minutes to allow the gel to solidify then Complete Crypt Medium without EGF and noggin, but with 10 µM Y-27632 and 100 ng/mL Wnt3a was overlaid on the cultures. Fresh EGF, noggin, and Rspo1 were added every 2 days and the medium was changed with Complete Crypt Medium every 4 days.

ISEMF transduction

Transduced ISEMF cell lines were created using short hairpin Rspo2 (shRspo2) or Rspo3 (shRspo3) lentiviruses. ISEMF cells were grown to 40% confluency on a 6-well plate and treated with the respective lentivirus for 24 hours. Successfully transduced cells expressed GFP and were subsequently FACS-sorted with a BD FACSAria cell sorter after one week of culture.

Implantation

Crypt-ISEMF co-cultures detached from the well around 7 days if the well was not pre-coated with gelatin prior to seeding the ISEMF. These detached cultures were used for the implantation studies. Non-woven polyglycolic acid felt scaffolds (Synthecon, Houston, TX) were sterilized with 80% ethanol for 30 minutes, rehydrated in decreasing concentrations of ethanol, and washed with sterile PBS. The sterile scaffolds were coated with neutralized Purecol collagen (Inamed Biomaterials, Fremont, CA) and allowed to dry. The detached crypt-ISEMF co-culture was suspended in Matrigel and seeded onto the scaffold. Adult wild type C57BL/6 mice were used as the recipients. A midline abdominal skin incision was made and the skin was raised to create a subcutaneous pocket for the scaffolds. The seeded side of the scaffold with the co-culture was placed against the abdominal muscle. The scaffold was sutured onto the muscle with 6-0 Prolene (Ethicon, Somerville, NJ) and the skin was closed. The scaffolds were retrieved 28 days after the implantation.

Histology

In vitro cultures and *in vivo* implants were fixed with 10% buffered formalin and processed for paraffin embedding. The blocks were cut into 5 μm slices and stained for hematoxylin and eosin. Antibody specific immunohistochemistry was performed using the Dako Autostainer system (Dako, Carpinteria, CA). Antibodies were purchased from Dako and used according to manufacturer protocol.

Immunofluorescence staining of the ISEMF was done directly in the well after fixation with 10% buffered formalin. The cells were permeabilized with 0.5% Triton-X (Sigma) in Tris buffer

solution and washed with 0.05% Tween 20 in PBS (EMD Chemicals, Gibbstown, NJ). Primary antibodies for α smooth muscle actin (SMA, Dako), desmin (Dako) and vimentin (Abcam, Cambridge, MA) were used at 1:50 dilutions and incubated over night at 4°C. Corresponding AlexaFluor 488 secondary antibodes (Invitrogen) were used at 1:200 dilutions and allowed to incubate for 30 minutes at room temperature. Vectashield with DAPI (Vector Labs, Burlingame, CA) was used to stain the nuclei of the cells. Images were taken on a Nikon Eclipse Ti microscope. (Nikon, Tokyo, Japan)

Enteroroid Measurements

Micrographs of the *in vitro* cultures were taken after 7 days using a Leica SP2 MP-FLIM microscope (Leica Microsystems, Buffalo Grove, IL). The microscope was configured to take 14 images at 5X magnification that covered the entire growth area. The images were assembled together and the composite large picture analyzed in ImageJ (NIH, Bethesda, MD) to count and measure the area of the enteroids. The colony forming efficiency was calculated by dividing the number of enteroids by the initial crypts seeded.

DNA/RNA isolation and qPCR

DNA and RNA were extracted and purified from the *in vitro* cultures on day 7 using the commercially available DNeasy and RNeasy kits (Qiagen, Valencia, CA), respectively. The quantitative real-time PCR reactions were prepared using the Quantitect Probe RT-PCR Kit (Qiagen). The primers and probe for GFP DNA were custom-designed and were purchased from

Eurofins MWG Operon (Huntsville, AL). The forward, reverse, and probe sequence are 5'-ACTACAACAGCCACAACGTCTATATCA-3', 5'-GGCGGATCTTGAAGTTCACC-3', and 5'-(6-FAM) CCGACAAGCAGAAGAACGGCATCA (Tamra-Q)-3', respectively. All RNA qPCR primers and probes were commercially available from Applied Biosystems. The qPCR reactions were prepared in MicroAmp Optical reaction plates (Applied Biosystems) and performed on an ABI Prism 7900 Sequence Detection System (Applied Biosystems). DNA qPCR results were analyzed using the without ISEMF group as a relative standard while for RNA, the analysis was done by the comparative C^T method using GAPDH as the housekeeping gene and whole small bowel as the normalizer (13).

RNA Deep Sequencing

RNA was isolated from B19 ISEMF and B20 cells, made into cDNA, built into a library, and sequenced. The generated data for each gene was converted to reads per kilobase per million mapped reads (RPKM) and compared as a fold change to B19. Adjusted p-values were calculated to designate significance between the comparisons and to account for false positives from multiple comparisons.

Results

ISEMF Characterization

Cultured organoids gave rise to elongated, fibroblastic cells. The identity of these cells was assessed by immunofluorescence and qPCR for α smooth muscle actin (Acta2), vimentin (Vim), and desmin (Des). Multiple lines of isolated cells (B18, B19, and B20) were tested, but all exhibited strong staining for α smooth muscle actin and vimentin but stained weakly for desmin (Figure 1A-C). The cells were also tested in co-culture with crypts in the absence of added soluble Rspo1. B18 and B19 showed enteroid growth, but B20 did not support the growth of the crypts. Without ISEMF and Rspo1, crypt cultures did not form enteroids and died within 2 days of plating. (Figure 1E) The qPCR of B19 cells confirmed the high expression of α smooth muscle actin and vimentin and an insignificant amount of desmin (Figure 1D). The B19 cells possessed characteristics of ISEMF and were used in the subsequent experiments.

Enteroid Growth in Co-Cultures

ISEMF were co-cultured with intestinal crypts isolated from the small intestine. In the presence of added soluble Rspo1 in the culture medium, crypts grown on top of ISEMF formed enteroids that were roughly 3 times larger at 59,600±13,400 μm^2 versus 19,400±13,400 μm^2 without ISEMF and had 6.1±2.7 times more epithelial DNA compared to crypts cultured without ISEMF (Figure 2, A-B). Crypts formed budding enteroids in both conditions, but they were larger and more complex in the presence of ISEMF (Figure 2, E-F). Crypts were also grown in a

configuration where they were suspended together with ISEMF in Matrigel, which yielded similar growth pattern as crypts grown on top of ISEMF (Figure 2, A-B,G).

When crypts were grown on a membrane that physically separated them from ISEMF, the enteroids were only about 1.5 times greater in size at 46,400±18,000 μm^2 compared to 29,900±10,900 μm^2 for crypts cultured on a membrane in the absence of ISEMF (Figure 3, A-B). Crypts grew into budding enteroids that increased in size and complexity in the presence of ISEMF (Figure 3, D-E).

The cultured crypts expressed high levels of Lgr5 mRNA in all growth configurations (Figure 2C, 3C). There was not a significant difference between crypts cultured with and without ISEMF ($p>0.28$). The cultured crypts also expressed differentiated epithelial markers but at a lower level compared to small intestine (Figure 2D, Figure 3C). The presence of mature epithelium was also confirmed by immunohistochemistry. E-cadherin (Figure 4C) and Cdx2 (Figure 4D) staining established that the enteroids were intestinal epithelium. Lysozyme (Figure 4E), synaptophysin (Figure 4F), and periodic acid-Schiff staining (Figure 4G) confirmed the presence of Paneth, enteroendocrine, and goblet cells, respectively. For most tested transcripts, there was not a statistically significant difference in mRNA expression between crypts cultured with and without ISEMF. However, lysozyme mRNA expression was notably 3 times higher in the co-culture crypts (Figure 2C). This difference was diminished when the co-cultures were spatially separated by a membrane (Figure 3C).

The colony forming efficiency was measured for the different growth configurations. There was not a significant difference between growing the crypts on top or mixed with ISEMF compared to without ISEMF. Similarly in the membrane separation condition, ISEMF did not make a difference in the colony forming efficiency.

In vivo Implantation

Crypts cultured on top of ISEMF spontaneously detached from tissue culture plastic that was not gelatin-coated. The detached co-cultures were placed on PGA woven scaffolds and were implanted subcutaneously to assess their *in vivo* growth. Crypts cultured in Matrigel without ISEMF were mechanically detached and were similarly placed on PGA woven scaffolds for implantation.

After 28 days of implantation, histology of the retrieved implants showed epithelial cyst formation (Figure 5A). Immunostaining demonstrated cells that expressed α smooth muscle actin around the epithelial cysts (Figure 5B). E-cadherin and Cdx2 were expressed in these cysts, confirming their intestinal epithelial origin (Figure 5, C-D). Moreover, positive staining for lysozyme, synaptophysin, and Periodic-acid Schiff suggests that cells in the cysts differentiated into Paneth cells, enteroendocrine cells, and goblet cells, respectively (Figure 5, E-G). Implants containing only cultured crypts without ISEMF did not yield any epithelial cysts (data not shown).

Enteroid Growth from Single Stem Cells

Lgr5-positive single cells were sorted from an Lgr5-GFP mouse and were grown in cultures with and without ISEMF. The Lgr5-positive cells showed greater growth under co-culture condition. The Lgr5-positive cells in co-culture with ISEMF grew into enteroids that covered about 3.5 times more total area per well at 353,000±18,700 μm^2 compared to 105,000±82,5000 μm^2 for single cells cultured without ISEMF (Figure 6A). Morphologically, the Lgr5-positive cells grew into budding enteroids regardless of the presence of ISEMF, but with different size and number of buds (Figure 6B). Immunohistochemistry of the co-cultures confirmed that ISEMF formed a layer of cells adjacent to the enteroids (Figure 7B). The enteroids also expressed Cdx2 and PAS, suggesting that single Lgr5-positive cells differentiated into mature intestinal epithelial cells (Figure 7, C-D).

Co-cultures of Lgr5-positive cells and ISEMF were placed on PGA scaffolds and were implanted subcutaneously. After 28 days, epithelial cysts were found in the retrieved implant with ISEMF surrounding the cysts (Figure 7, E-F). Cdx2 immunostaining verified the intestinal origin of the cysts (Figure 7G).

RNA Deep Sequencing

RNA deep sequencing was performed on the B19 ISEMF and B20 cells to identify differences at the transcript level. Notable genes that were highly expressed in B19 but not B20 are listed in Figure 9.

Modified ISEMF

Aside from the enhancing effects on the growth of intestinal crypts and single cells, ISEMF are able to support enteroid growth when the Wnt agonist R-spondin1 (Rspo1) was eliminated from the culture medium (Figure 1E). However, cultures of crypts and single cells without ISEMF and Rspo1 did not grow into enteroids. B19 ISEMF were compared to the B20 cells, which did not support growth without Rspo1, for mRNA expression of Rspo1, Rspo2, and Rspo3. Neither cells expressed high levels of Rspo1 and Rspo3, but B19 ISEMF did highly express Rspo2 compared to B20 cells (Figure 8A). Short-hairpin Rspo2 (shRspo2) and Rspo3 (shRspo3) vectors were created to transduce the ISEMF to reduce the expression of Rspo2 and Rspo3 in ISEMF (Figure 8, B-C).

When such transduced ISEMF were co-cultured with crypts without added Rspo1, a 25% reduction in enteroid growth was found when the transduced ISEMF were employed in place of normal ISEMF.

Discussion

In this study, we showed that co-cultures of crypts or intestinal stem cells and ISEMF result in larger enteroids than cultures without ISEMF. However, there was no significant effect on the number of enteroids that formed. Moreover, ISEMF are capable of sustaining the growth of enteroids subcutaneously *in vivo* without external intervention or addition of growth factors. This represents a significant improvement in culturing stem cells for study or tissue engineering applications.

The results suggest that the effect on the enteroids is due to growth factors produced by ISEMF. Direct cell-to-cell contact between the ISEMF and epithelial cells is not necessary for the beneficial effect. However, as the distance to the epithelial cell is increased, the effect diminishes. It is possible that a soluble factor with a short effective half-life limits the range of interaction. We have tried to test this hypothesis (data not shown) by growing crypts with conditioned media from ISEMF cultures, but the crypts did not survive in conditioned media without exogenous Rspo1. It is unknown if cross-talk between the stem cells and ISEMF is necessary to promote the growth stimulating effect.

The ability to grow in the absence of exogenous Rspo1 is one of the advantages of ISEMF co-cultures. Rspo1 is an agonist of the Wnt pathway, which has been established as the proliferative pathway for IESCs. (14, 15) Previously described culture systems require exogenous Rspo1 for crypt or stem cell survival. (4, 6) mRNA qPCR analysis of the ISEMF showed negligible gene expression of Rspo1 compared to small bowel. However, RNA deep sequencing of the B19

ISEMF revealed high levels of Rspo2 compared to B20, the myofibroblast-like cells that did not support growth of the crypts without Rspo1. Rspo2 has been reported to bind to Lgr5 and its homologues, which are components of the Wnt pathway. (16) Knockdown of Rspo2 expression with short hairpin RNA showed a reduction in gene expression and enteroid growth in co-cultures without exogenous Rspo1, but did not eliminate it completely. The partial knockdown of Rspo2 may explain why crypts still survived in the co-cultures. Rspo3 was also expressed in ISEMF and our short hairpin RNA vector was able to knock it down completely and reduce enteroid growth in co-culture. Rspo2 and Rspo3 may contribute to the interaction, but it may not be limited to only these factors. For example, Rspo4 is another R-spondin analog, but was not tested. It is unknown if adding exogenous Rspo2, Rspo3, or Rspo4 can substitute Rspo1 or ISEMF in crypt cultures. R-spondin2 is a promising candidate responsible for signaling between ISEMF and stem cells, but further investigation of the different R-spondin analogs is necessary.

Aside from producing R-spondins, ISEMF may also affect the Wnt pathway through Paneth cells. Paneth cells have been reported to provide Wnt signals for stem cell survival (9) and crypts cultured with ISEMF expressed higher lysozyme than without. The finding suggests that the myofibroblasts upregulate differentiation of stem cells into Paneth cells and indirectly increase Wnt signals for stem cell growth. Tight regulation of Paneth cells is necessary to maintain the optimal level of contact between them and the stem cells in the niche (9) and ISEMF may have a role in the regulation.

The RNA sequencing of the B19 ISEMF and B20 cells reveals several additional potential modes of regulation. Sfrp4 and Frzb (also known as Sfrp3) are part of a family of proteins known

to be Wnt inhibitors and are highly expressed in B19 but not B20. Recent reports have found them to be more complex and possibly linked to enhanced Wnt signaling (17, 18). In the kidney, Sfrp1 alone was found to inhibit Wnt4, but Sfrp2 blocked the effect of Sfrp1 and in turn enhanced the Wnt signal (17). It is unclear how these molecules interact in the intestinal setting, but it is an area worth investigating. Aside from modulators of the Wnt pathway, the ISEMF also highly expressed Hhip, an inhibitor of the hedgehog pathway. Knockouts of hedgehog ligands, Shh and Ihh, in mice have resulted in enhanced or reduced intestinal epithelial growth, respectively (19). Low level of inhibition of the pathway with Hhip increased epithelial proliferation, but deformed villus development in mice (20). Similarly, ISEMF could be causing a proliferative state in the epithelial cells through hedgehog inhibition.

Our *in vitro* findings provide support for the use of ISEMF in *in vivo* applications of intestinal stem cells. Previous studies from our laboratory that have shown *in vivo* epithelial growth have used intestinal organoids that contain crypts and its surrounding mesenchyme (21). These studies re-implant the organoids upon extraction without *in vitro* expansion (22, 23). These organoid-based approaches result in a functional neomucosa but have limited clinical use since they need a lot of starting material to generate a small amount of mucosa. In contrast, we have shown in our current study that it is possible to subculture and expand intestinal enteroids and ISEMF *in vitro*. Subcutaneous implantation of the co-cultures has resulted in epithelial cysts that contain Paneth, goblet, and enteroendocrine cells. However, there is no epithelial growth when only enteroids are implanted, which is likely due to the absence of vital growth factors such as Rspo1 in the subcutaneous environment. Immunohistochemistry staining for α smooth muscle actin on the explants reveals that ISEMF encircle the cysts. The close proximity resembles the natural setting

where ISEMF lie just basal to the crypts, which is likely a determining factor for the survival of the epithelial cells. Other configurations such as scaffolds seeded with co-cultures mechanically scraped from the plate did not yield viable epithelium. (data not shown) The detached co-cultures contract and keep the enteroids enclosed within a layer of ISEMF and its implantation procedure does not disrupt the established matrix. The finding emphasizes the importance of ISEMF and their orientation with the epithelium.

The results present an exciting direction for the development of intestinal tissue engineering. Clinical application for short bowel syndrome would require several feet of tissue engineered intestine to overcome the deficiency so it would be necessary to expand the intestinal components *in vitro* prior to combining them for *in vivo* treatment. There have been advancements in culturing intestinal smooth muscle (24) and enteric cells (25) and our study has provided the viability of ISEMF and epithelium co-cultures. Moreover, our *in vivo* co-culture system does not require external intervention such as the delivery of growth factors. The host vascular system provides the basic nutrients and the ISEMF are capable of maintaining the epithelial stem cells. An ideal tissue engineered intestine would be self-sustaining in the *in vivo* setting. Previous literature has shown that vascular smooth muscle and endothelial cells can be grown on multilayered electrospun scaffolds and to form blood vessels. (26) A similar scaffold can be adopted for use with intestinal smooth muscle, ISEMF, and intestinal epithelial cells.

Conclusion

This study has demonstrated that ISEMF and epithelial stem cell co-cultures produce larger enteroids and improve their viability even in the absence of Rspo1. Similarly, the effect can be reproduced in subcutaneous *in vivo* implants. The findings suggest that ISEMF may produce soluble factors that interact with the IESC and promote their growth. Adapting ISEMF and IESC into a functional tissue engineered intestine will be the next major challenge in developing a clinical application for diseases like short bowel syndrome.

Future Direction

The beneficial applications of ISEMF make it a subject of interest and more research needs to be done to fully characterize them. Elucidating the biomolecular pathways between ISEMF and IESC will be critical to understanding the interaction. The deep sequencing data can be repeated and closely studied to identify genes that contribute to the pathways. Additional knockdown experiments in the ISEMF or transgenic mice with the chosen genes would help prove the functions of the genes.

Moreover, additional work can be done to improve the *in vivo* model for tissue engineering. The physical limitations of the interaction are worth investigating. We found that 1 mm causes a diminished effect, but smaller distances between the IESC and ISEMF can be experimented to determine the lower limit on the interaction. This knowledge will help with the design of scaffolds and seeding of the cells. Additionally, we have been experimenting with matrices other than Matrigel, such as collagen. The components in Matrigel are not well defined and would not be applicable in a clinical setting (27). Furthermore, one of the first major steps in intestinal tissue engineering would be to grow sheets of epithelium rather than enteroids. The matrix stiffness and growth factor components will likely determine the structure of the epithelium. Finally, further co-culture experiments with other intestinal cells such as smooth muscle and interstitial cells of Cajal will be necessary to study their synergistic interactions and functionality in the engineered intestine.

Figures

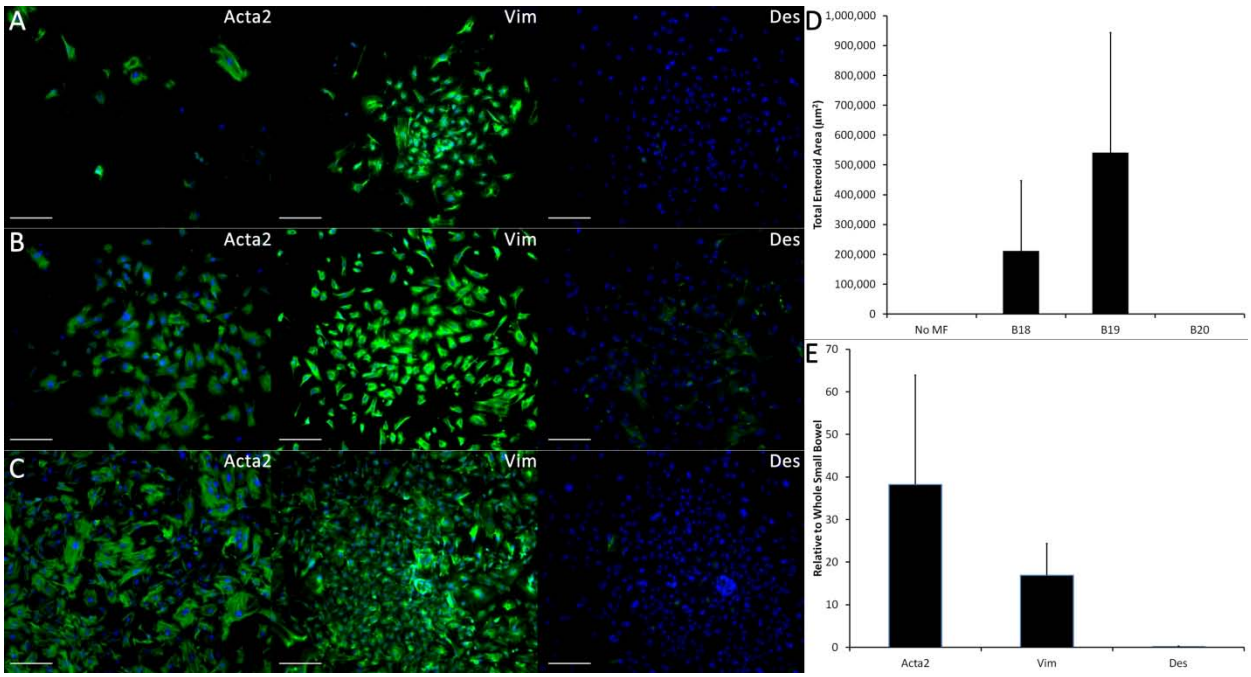

Figure 1: Characterization of ISEMF

Isolated ISEMF were characterized through immunofluorescent staining and mRNA qPCR. The (A) B18, (B) B19, and (C) B20 cells were stained for α smooth muscle actin (Acta2), vimentin (Vim), and desmin (Des). (D) ISEMF lines were also assessed by their ability to sustain intestinal crypt cultures without R-spondin1 in the culture media. The total area of the enteroids per well was measured for each line and without ISEMF (n=2). (E) Quantitative RT-PCR was performed on the B19 ISEMF mRNA lysate using the same markers and normalized to small bowel (n=4). The scale bar represents 200 µm.

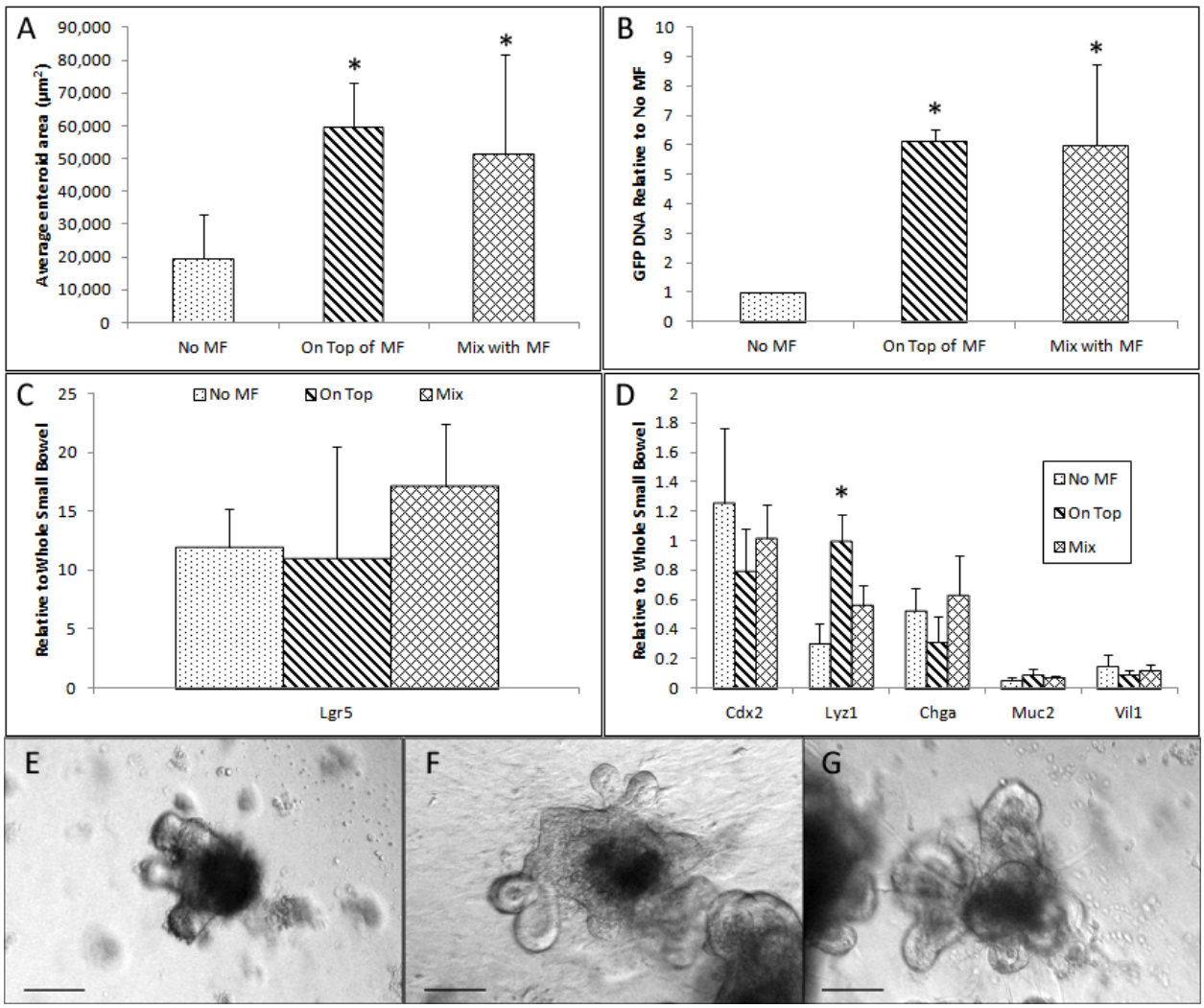

Figure 2: Epithelial crypt and ISEMF co-cultures with direct contact.

(A) Average area of an enteroid in the *On Top* and *Mix* co-culture conditions were measured and compared to no ISEMF (n=5). (B) GFP DNA qPCR was used as a measurement of total epithelial growth. Cultures on top or mixed with ISEMF were normalized to cultures without ISEMF (n=7). mRNA expression of (C) Lgr5 and (D) differentiated epithelial markers was assessed by qPCR and normalized to whole small bowel (n=3). Light microscope images of an (E) enteroid without ISEMF, (F) on top, and (G) mixed with ISEMF were captured at day 7. The scale bar represents 100 µm. Asterisk indicates $p<0.05$ when compared to *No MF*.

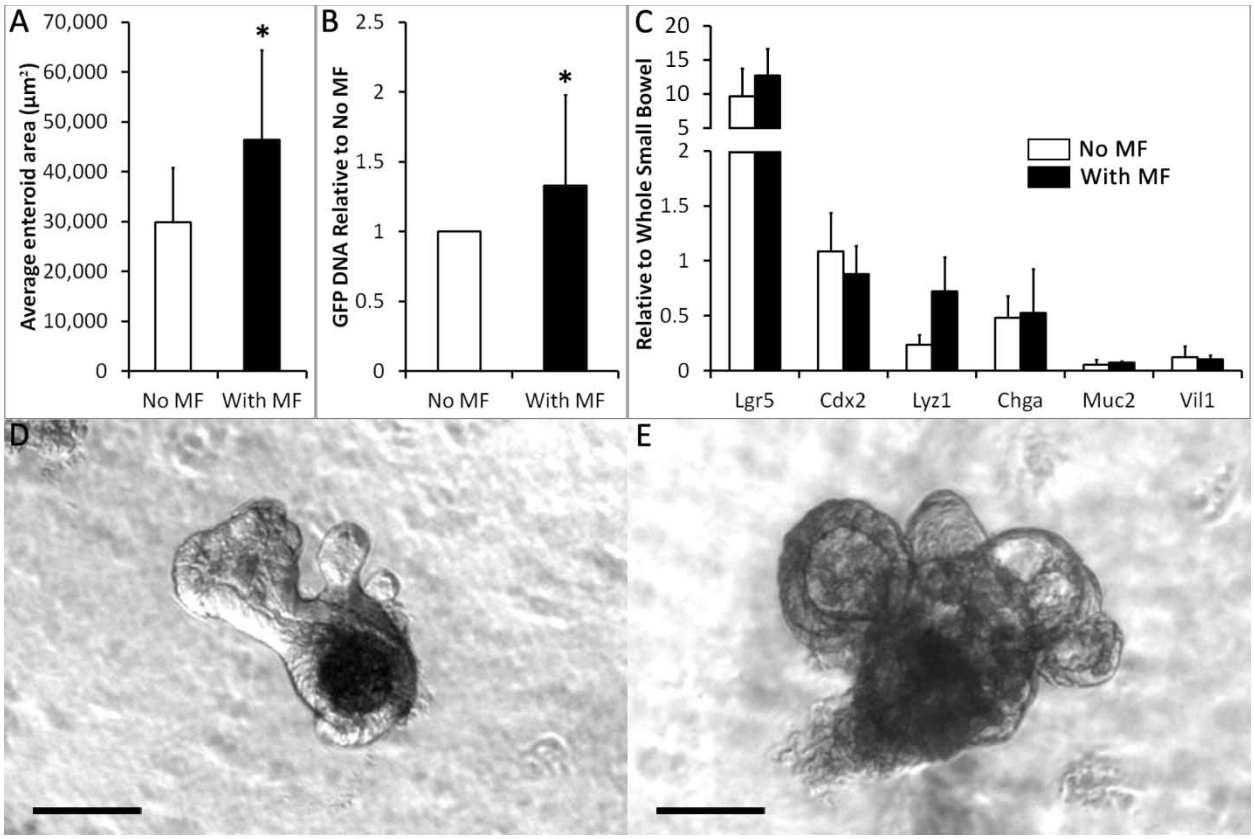

Figure 3: Epithelial crypt and ISEMF co-cultures separated by a membrane.

(A) The average area an enteroid was measured on cultures grown on a semi-permeable membrane with or without ISEMF in the well beneath it (n=5). (B) GFP DNA was quantified with qPCR to measure epithelial growth (n=7). (C) mRNA expression of Lgr5 and differentiated epithelial markers was assessed by qPCR and normalized to whole small bowel (n=3). Light microscope images an (E) enteroid without ISEMF and (F) with ISEMF below the membrane were captured at day 7. The scale bar represents 100 µm. Asterisk indicates $p<0.05$ when compared to *No MF*.

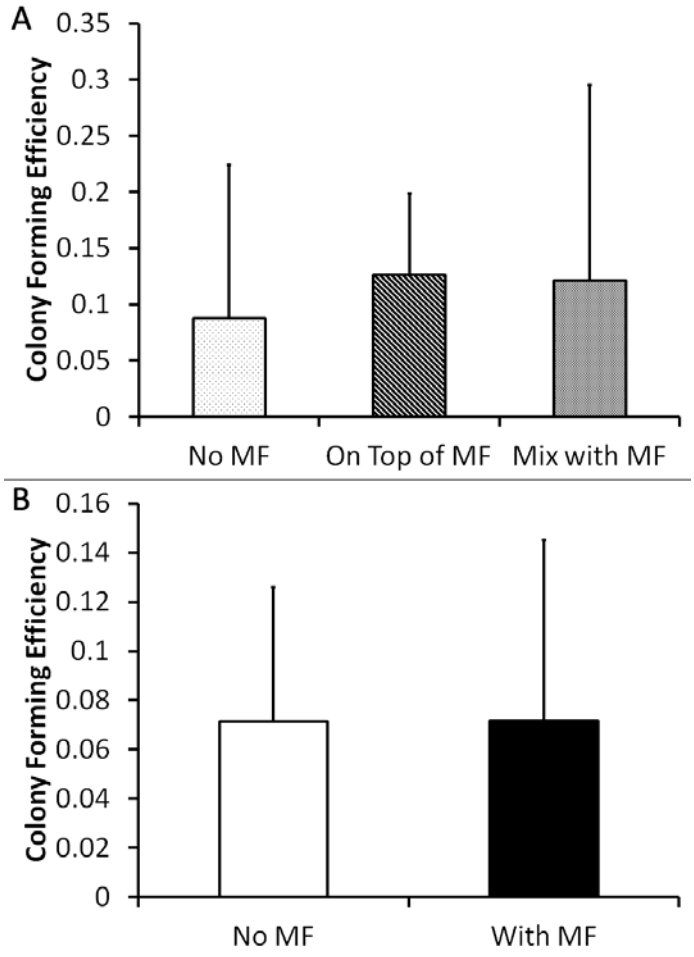

Figure 4: Colony forming efficiency of co-cultures

The colony forming efficiency was measured for the (A) direct contact (n=5) and (B) membrane-separated (n=5) co-culture conditions by dividing the number of enteroids at day 7 by the number of crypts initially seeded.

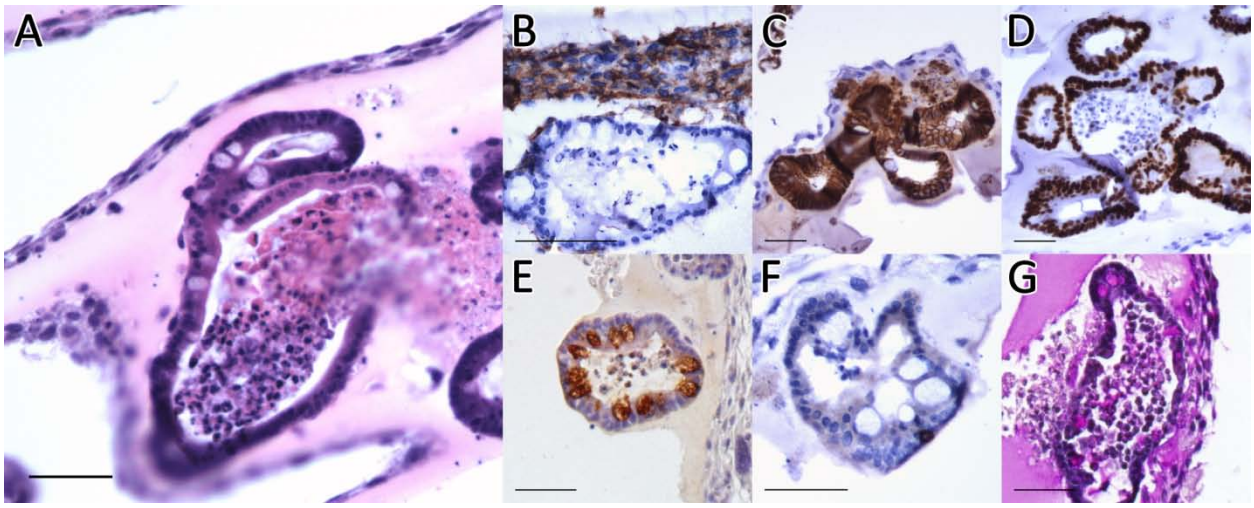

Figure 5: Histology of *in vitro* co-cultures on top of ISEMF after 7 days

Immunohistochemistry staining of the co-cultures for (A) hematoxylin and eosin (H&E), (B) α smooth muscle actin, (C) e-cadherin, (D) cdx2, (E) lysozyme, (F) synaptophysin, and (G) periodic acid-Schiff (PAS). The scale bar represents 50 µm.

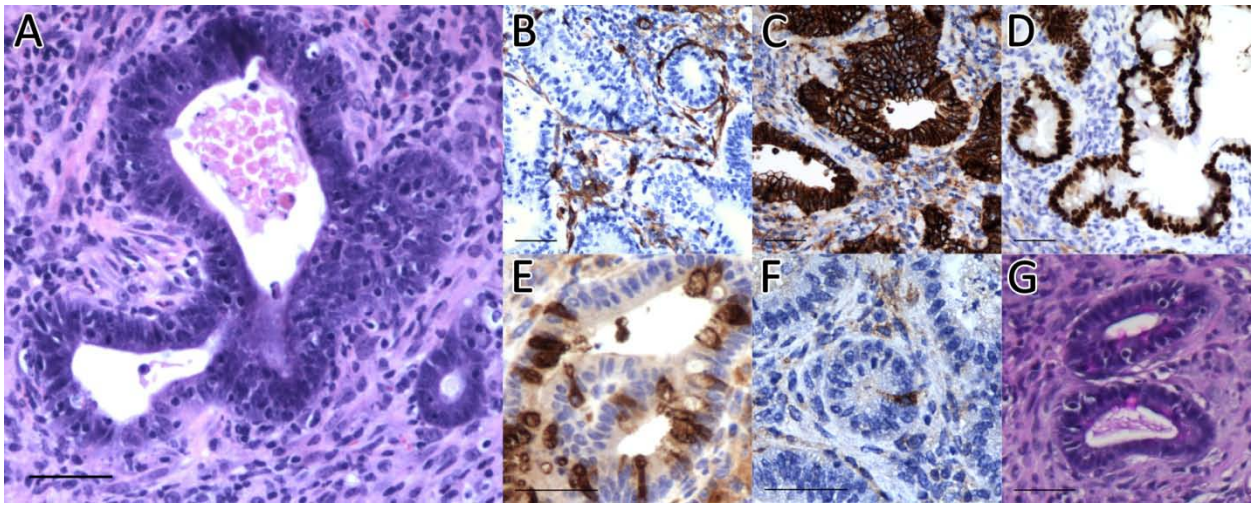

Figure 6: Histology of co-culture *in vivo* implants after 28 days.

Immunohistochemisty staining of the retrieved implants for (A) H&E, (B) α smooth muscle actin, (C) e-cadherin, (D) cdx2, (E) lysozyme, (F) synaptophysin, and (G) PAS. The scale bar represents 50 µm.

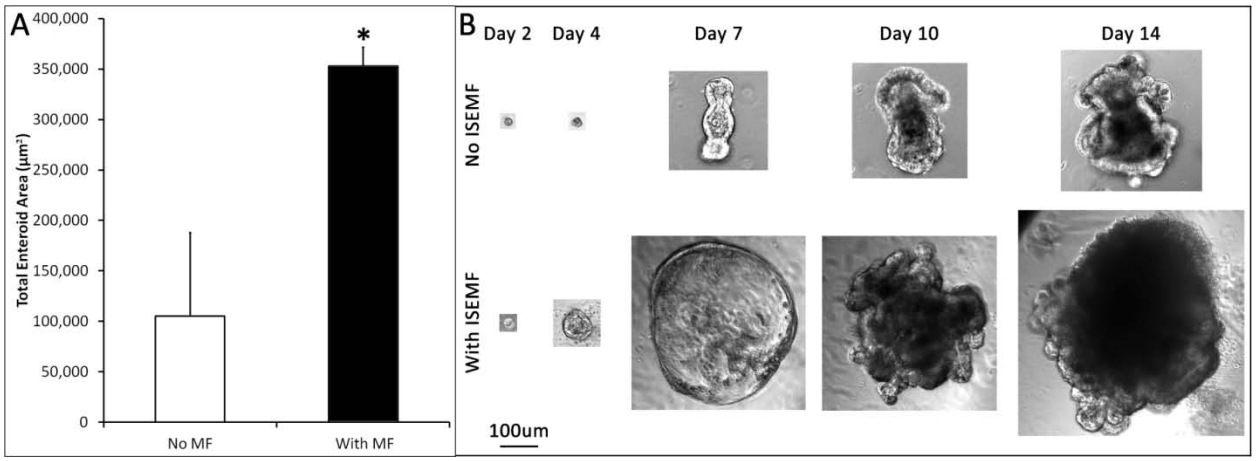

Figure 7: *In vitro* culture of single sorted stem cells

(A) The total area of the enteroids per well was measured to quantify the growth of the stem cells with and without ISEMF (n=2). (B) Time lapse images of the growth up to day 14. The scale bar represents 100 µm. Asterisk indicates $p<0.05$ when compared to *No MF*.

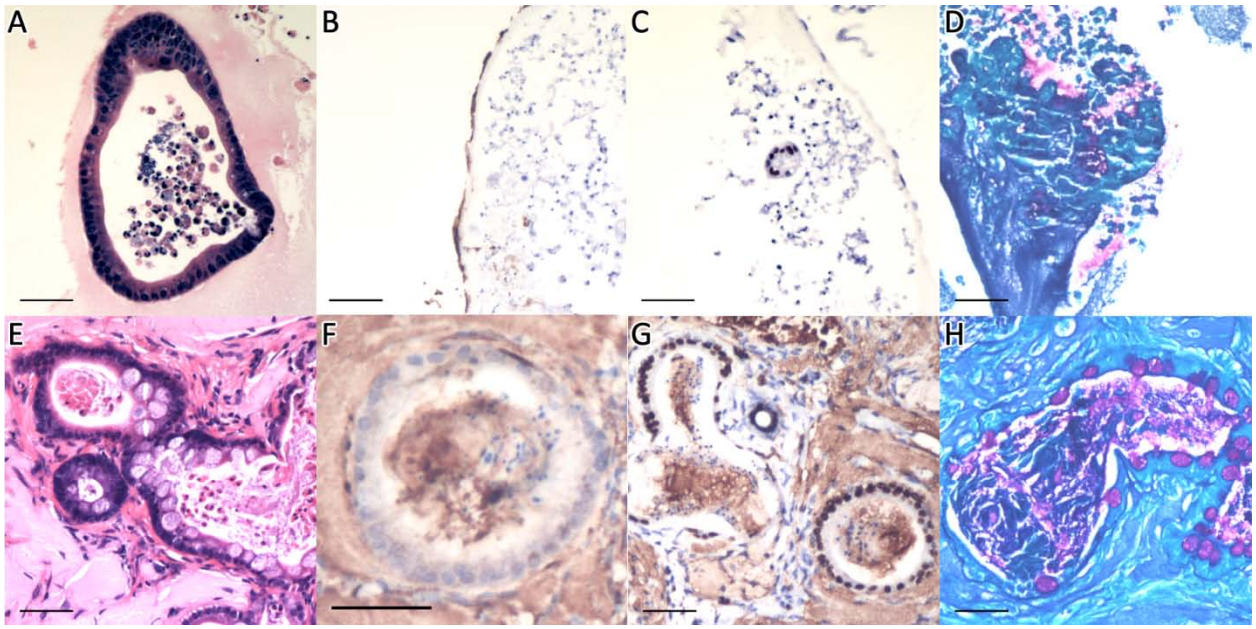

Figure 8: Histology of the *in vitro* and *in vivo* stem cell co-cultures

Immunohistochemistry staining of the single cells grown *in vitro* and implanted *in vivo* for (A,E) H&E, (B,F) α smooth muscle actin, (C,G) cdx2, and (D,H) PAS, respectively. The scale bar represents 50 µm.

Gene	Description	B19 RPKM	B20 RPKM	log2 Fold Change	Adjusted p-value
Hhip	Hedgehog-interacting protein	132.71	0.06	-11.11	2.34E-13
Lgr5	leucine rich repeat containing G protein coupled receptor 5	77.70	0.05	-10.71	6.62E-14
Rspo2	R-spondin 2 homolog (Xenopus laevis)	268.13	0.97	-8.07	2.75E-10
Sfrp4	secreted frizzled-related protein 4	152.54	1.15	-7.02	1.28E-08
Crip1	cysteine-rich protein 1 (intestinal)	166.85	2.32	-6.14	7.66E-04
Wisp2	WNT1 inducible signaling pathway protein 2	204.62	6.27	-5.00	4.74E-05
Lama2	laminin, alpha 2	60.08	3.25	-4.17	6.00E-04
Frzb	frizzled-related protein	31.04	1.70	-4.16	9.93E-03
Hgf	hepatocyte growth factor	90.25	9.14	-3.27	2.53E-02
Lama5	laminin, alpha 5	30.02	3.27	-3.16	2.26E-02

Figure 9: RNA sequencing data of ISEMF for select genes

mRNA from B19 ISEMF and B20 cells was made into a cDNA library and analyzed through RNA deep sequencing. The raw data was converted to reads per kilobase per million mapped reads (RPKM). Negative values in fold change signify more cDNA in the B19 cells. The adjusted p-value accounts for multiple comparisons.

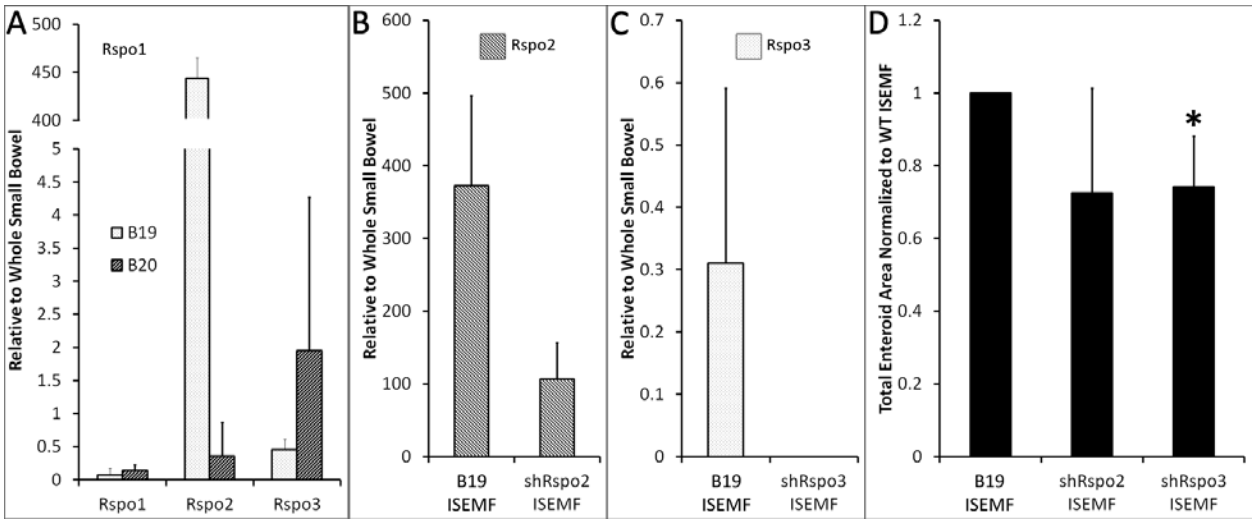

Figure 10: Growth of Enteroids on R-spondin silenced ISEMF

(A) Rspo1, Rspo2, and Rspo3 mRNA expression was assessed for B19 and B20 cells (n=2). B19 ISEMF were transduced with shRspo2 or shRspo3 vectors and the resulting cells were measured for (B) Rspo2 (n=2), and (C) Rspo3 (n=2) mRNA expression. (D) ShRspo2 and shRspo3 transduced ISEMF were grown with crypts in the absence of exogenous Rspo1 in the culture media. At day 7, the total enteroid area per well was measured and normalized to the growth on B19 ISEMF (n=4). Asterisk indicates $p<0.05$ when compared to *B19 ISEMF*.

References

1. Barker N, Oudenaarden A Van, Clevers H (2012) Perspective Identifying the Stem Cell of the Intestinal Crypt: Strategies and Pitfalls. *Cell Stem Cell* 11:452–460.

2. Yeung TM, Chia L a, Kosinski CM, Kuo CJ (2011) Regulation of self-renewal and differentiation by the intestinal stem cell niche. *Cellular and molecular life sciences : CMLS* 68:2513–23.

3. Barker N et al. (2007) Identification of stem cells in small intestine and colon by marker gene Lgr5. *Nature* 449:1003–7.

4. Sato T et al. (2009) Single Lgr5 stem cells build crypt-villus structures in vitro without a mesenchymal niche. *Nature* 459:262–5.

5. Korinek V et al. (1998) Depletion of epithelial stem-cell compartments in the small intestine of mice lacking Tcf-4. *Nature genetics* 19:379–83.

6. Gracz AD, Puthoff BJ, Magness ST (2012) Identification, Isolation, and Culture of Intestinal Epithelial Stem Cells from Murine Intestine. *Methods in Molecular Biology* 879:89–107.

7. Draper JS, Moore HD, Ruban LN, Gokhale PJ, Andrews PW (2004) Culture and characterization of human embryonic stem cells. *Stem cells and development* 13:325–36.

8. Powell DW et al. (1999) Myofibroblasts. II. Intestinal subepithelial myofibroblasts. *The American journal of physiology* 277:C183–201.

9. Sato T et al. (2011) Paneth cells constitute the niche for Lgr5 stem cells in intestinal crypts. *Nature* 469:415–8.

10. Fritsch C et al. (2002) Epimorphin expression in intestinal myofibroblasts induces epithelial morphogenesis. *The Journal of Clinical Investigation* 110:1629–1641.

11. Evans GS, Flint N, Somers a S, Eyden B, Potten CS (1992) The development of a method for the preparation of rat intestinal epithelial cell primary cultures. *Journal of cell science* 101 (Pt 1:219–31.

12. Plateroti M et al. (1998) Subepithelial fibroblast cell lines from different levels of gut axis display regional characteristics. *American journal of physiology. Gastrointestinal and liver physiology* 274:G945–54.

13. Schmittgen TD, Livak KJ (2008) Analyzing real-time PCR data by the comparative CT method. *Nature Protocols* 3:1101–1108.

14. Kim K-A et al. (2005) Mitogenic influence of human R-spondin1 on the intestinal epithelium. *Science (New York, N.Y.)* 309:1256–9.

15. Van der Flier LG, Clevers H (2009) Stem cells, self-renewal, and differentiation in the intestinal epithelium. *Annual review of physiology* 71:241–60.

16. De Lau W et al. (2011) Lgr5 homologues associate with Wnt receptors and mediate R-spondin signalling. *Nature* 476:293–7.

17. Bovolenta P, Esteve P, Ruiz JM, Cisneros E, Lopez-Rios J (2008) Beyond Wnt inhibition: new functions of secreted Frizzled-related proteins in development and disease. *Journal of cell science* 121:737–46.

18. Von Marschall Z, Fisher LW (2010) Secreted Frizzled-Related Protein-2 (sFRP2) Augments Canonical Wnt3a-induced Signaling. *Biochemical and biophysical research communications* 400:299–304.

19. Ramalho-Santos M, Melton D a, McMahon a P (2000) Hedgehog signals regulate multiple aspects of gastrointestinal development. *Development (Cambridge, England)* 127:2763–72.

20. Madison BB et al. (2005) Epithelial hedgehog signals pattern the intestinal crypt-villus axis. *Development (Cambridge, England)* 132:279–89.

21. Avansino JR, Chen DC, Hoagland VD, Woolman JD, Stelzner M (2006) Orthotopic transplantation of intestinal mucosal organoids in rodents. *Surgery* 140:423–34.

22. Agopian VG, Chen DC, Avansino JR, Stelzner M (2009) Intestinal stem cell organoid transplantation generates neomucosa in dogs. *Journal of gastrointestinal surgery : official journal of the Society for Surgery of the Alimentary Tract* 13:971–82.

23. Chen DC et al. (2006) Comparison of polyester scaffolds for bioengineered intestinal mucosa. *Cells, tissues, organs* 184:154–65.

24. Lee M, Wu BM, Stelzner M, Reichardt HM, Dunn JCY (2008) Intestinal smooth muscle cell maintenance by basic fibroblast growth factor. *Tissue engineering. Part A* 14:1395–402.

25. Geisbauer CL, Wu BM, Dunn JCY (2012) Transplantation of enteric cells into the aganglionic rodent small intestines. *The Journal of surgical research* 176:20–8.

26. Ju YM, Choi JS, Atala A, Yoo JJ, Lee SJ (2010) Bilayered scaffold for engineering cellularized blood vessels. *Biomaterials* 31:4313–21.

27. Kleinman HK, Martin GR (2005) Matrigel: basement membrane matrix with biological activity. *Seminars in cancer biology* 15:378–86.